

# **$\beta$ -Silyl-Substituted Silaadamantyl, Silabicyclo[2.2.2]octyl, Silanorbornyl, and 1-Silacyclohexyl Cations. A Theoretical (DFT and GIAO NMR) Study**

Takao Okazaki<sup>†,‡</sup> and Kenneth K. Laali<sup>\*,†</sup>

Department of Chemistry, Kent State University, Kent, Ohio 44242, and  
Department of Energy and Hydrocarbon Chemistry, Kyoto University, Kyoto, Japan

*klaali@kent.edu*

Received August 13, 2002

Parent 1-silaadamant-1-yl (**1<sup>+</sup>**) and a series of mono- $\beta$ -silyl-substituted- (**2-Me<sup>+</sup>**, **2-F<sup>+</sup>**, **2-Cl<sup>+</sup>**, **2-Br<sup>+</sup>**), bis- $\beta$ -silyl-substituted- (**3-Me<sup>+</sup>**), and tris- $\beta$ -silyl-substituted (**4-Me<sup>+</sup>**)-1-silaadamant-1-yl cations were studied by the DFT method at the B3LYP/6-31G(d,p) level and by GIAO NMR at the B3LYP/6-31G(d,p)//B3LYP/6-31G(d,p) level. The geometries, relative energies, NMR chemical shifts, and charge distribution in the bridgehead silylum ions are discussed and compared. The magnitude of the  $\beta$ -silyl effect (the Si–C–Si<sup>+</sup> hyperconjugation) is gauged as a function of structure. Related model studies on the silabicyclo[2.2.2]octyl (**5<sup>+</sup>**, **6<sup>+</sup>**, **5a<sup>+</sup>**, and **6a<sup>+</sup>**), silanorbornyl (**7<sup>+</sup>** and **8<sup>+</sup>**), and silacyclohexyl cations (**9<sup>+</sup>** and **10<sup>+</sup>**) were carried out in which the effect of  $\beta$ -silyl substitution on geometry, stability, and NMR chemical shifts was probed. The acyclic model Me<sub>3</sub>Si–CH<sub>2</sub>–Si<sup>+</sup>(Me)<sub>2</sub> (**11<sup>+</sup>**) was used to gauge the influence of the twist angle between the p-orbital at Si<sup>+</sup> and the C–Si bond on relative stability and on the changes in the <sup>29</sup>Si NMR chemical shifts. Finally, interaction of **1<sup>+</sup>** with H<sub>2</sub>O and MeOH and **2-Me<sup>+</sup>** with H<sub>2</sub>O was also examined. The resulting optimized structures (**12<sup>+</sup>**, **13<sup>+</sup>**, and **14<sup>+</sup>**) and the computed NMR chemical shifts are most compatible with the formation of silaoxonium ions.

## Introduction

Following Jorgenson's lead,<sup>1</sup> a number of theoretical studies have examined the origin and the magnitude of the  $\beta$ -silicon effect in carbenium ions.<sup>2,3</sup> Hyperconjugative stabilization between the  $\beta$ -Si–C and the carbocation center, i.e., the stereoelectronic effect, also termed vertical stabilization, has been recognized as a principal factor, with inductive and polarization effects contributing to a lesser extent. An authoritative recent review covering theoretical, stable ion, and solvolytic studies has summarized the progress in silyl-substituted carbocations.<sup>4</sup> The novel bis- $\beta$ -silyl-substituted vinyl cations and bis-silylated benzenium ions are the latest additions to the family of  $\beta$ -silylated carbocations.<sup>5,6</sup> In comparison, there are fewer studies on  $\beta$ -silylated silylum ions in general

and on the  $\beta$ -silyl effect on silylum ions in particular. In agreement with theory that predicted diminishing importance of  $\pi$ -conjugation in Si–C–Si<sup>+</sup> as compared to Si–C–C<sup>+</sup>,<sup>2b</sup> the kinetics of hydride abstraction from silane by trityl cation demonstrated diminished hyperconjugative stabilization for the silylum ions as compared to carbenium ions.<sup>7</sup>

Geometrical constraints and rigidity in the silaadamantane ring system make it an interesting probe for studying hyperconjugation. Sequential addition of  $\beta$ -silicon atoms at the bridgehead positions provides the opportunity to study their stepwise effects on relative stability, geometry, NMR features, and charge distribution in bridgehead silylum ions.

In relation to a recent synthetic study focusing on the 1,3,5,7-tetrasilaadamantane skeleton and the chemoselective synthesis of the mono- and bis-silyl triflates from 1,3,5,7-tetramethyl-1,3,5,7-tetrasilaadamantane (Figure 1),<sup>8</sup> and in connection to a DFT study of the 1,3-dehydro-silaadamantyl dications,<sup>9</sup> we have conducted a DFT study on the silaadamantyl, silabicyclo[2.2.2]octyl, silanorbornyl, and silacyclohexyl cations.

(7) Basso, N.; Gors, S.; Popowski, E.; Mayr, H. *J. Am. Chem. Soc.* **1993**, *115*, 6025.

(8) (a) Laali, K. K.; Koser, G. F.; Huang, S. D.; Gangoda, M. *J. Organomet. Chem.* **2002**, *658*, 141. (b) Formation of a donor–acceptor complex between 1-bromo-3,5,7-trimethyl-1,3,5,7-tetrasilaadamantane and AlBr<sub>3</sub> had earlier been reported, see: Olah, G. A.; Field, L. D. *Organometallics* **1982**, *1*, 1485.

(9) Okazaki, T.; Galembeck, S. E.; Laali, K. K. *J. Org. Chem.* **2002**, *67*, 8721.

<sup>†</sup> Kent State University.

<sup>‡</sup> Kyoto University.

(1) Wierschke, S. G.; Chandrasekhar, J.; Jorgensen, W. L. *J. Am. Chem. Soc.* **1985**, *107*, 1496.

(2) Review chapters: (a) Apeloig, Y. In *The Chemistry of Organic Silicon Compounds*; Patai, S., Rappoport, Z., Eds.; Wiley: New York, 1989; Chapter 2. (b) Apeloig, Y. In *Heteroatom Chemistry*; Block, E., Ed.; VCH: New York, 1990; Chapter 2.

(3) Other review summaries (a) Prakash, G. K. S. In *Stable Carbocation Chemistry*; Prakash, G. K. S., Schleyer, P. v. R., Eds.; Wiley: New York, 1997; Chapter 4. (b) Olah, G. A.; Laali, K. K.; Wang, Q.; Prakash, G. K. S. *Onium Ions*; Wiley: New York, 1998; Chapter 9. (4) Siehl, H.-U.; Müller, T. In *The Chemistry of Organic Silicon Compounds*; Rappoport, Z., Apeloig, Y., Eds.; Wiley: Chichester, 1998; Vol. 2, Part 1, Chapter 12.

(5) Müller, T.; Meyer, R.; Lennartz, D.; Siehl, U.-H. *Angew. Chem., Int. Ed.* **2000**, *39*, 3074.

(6) Meyer, R.; Werner, K.; Müller, T. *Chem. Eur. J.* **2002**, *8*, 1163.

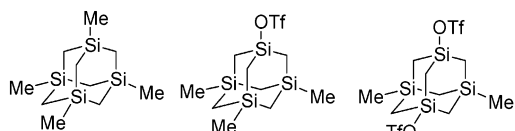


**FIGURE 1.** Silaadamantyl substrates from previous study.

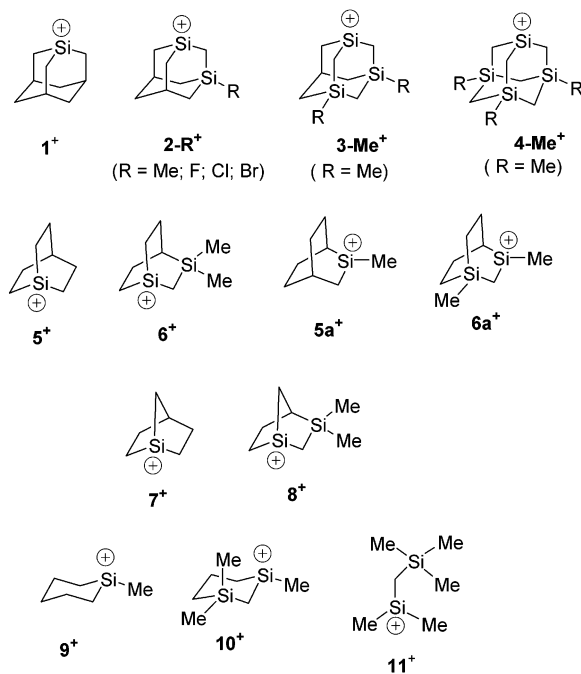


**FIGURE 2.** Silaadamantyl cations, silabicyclo[2.2.2]octyl cations, silanorbornyl cations, silacyclohexyl cations, and an acyclic model  $\text{Me}_3\text{Si}-\text{CH}_2-\text{Si}^+(\text{Me})_2$ .

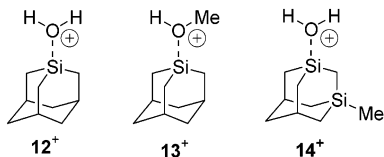


**FIGURE 3.** Model study of 1-silaadamantyl cation  $1^+$  with  $\text{H}_2\text{O}$  ( $12^+$ ) and  $\text{MeOH}$  ( $13^+$ ) and its  $\beta$ -silyl-substituted derivative  $2\text{-Me}^+$  with  $\text{H}_2\text{O}$  ( $14^+$ ).

Relative energies, geometrical features, manifestation and magnitude of hyperconjugative stabilization as a function of structure, GIAO NMR chemical shifts, and charge localization mode in the corresponding  $\beta$ -silylated silylium ions have been examined and compared. Influence of the twist angle between the p-orbital of  $\text{Si}^+$  and the  $\text{C}-\text{Si}$  bond in the acyclic model  $\text{Me}_3\text{Si}-\text{CH}_2-\text{Si}^+(\text{Me})_2$  was probed, and interactions of the silaadamantyl cations ( $1^+$  and  $2\text{-Me}^+$ ; see Figure 2) with  $\text{H}_2\text{O}$  and with  $\text{MeOH}$  were also examined.

## Results and Discussion

Structures (Figures 2 and 3) were optimized by using molecular point groups  $C_{3v}$  for  $1^+$ ,  $C_s$  for  $2\text{-Me}^+$ ,  $2\text{-F}^+$ ,  $2\text{-Cl}^+$ ,  $2\text{-Br}^+$ ,  $3\text{-Me}^+$ ,  $7^+$ ,  $9^+$ , and  $12^+$ ,  $C_{3v}$  for  $4\text{-Me}^+$ ,  $C_3$  for  $5^+$ , and  $C_1$  for  $5a^+$ ,  $6^+$ ,  $6a^+$ ,  $8^+$ ,  $10^+$ ,  $11^+$ ,  $13^+$ , and  $14^+$  by the DFT method at the B3LYP/6-31G(d,p) level, using the Gaussian 98 package.<sup>10</sup> The corresponding neutral

silanes  $1-11$ , silanols  $12$  and  $14$ , and silyl ether  $13$  were also calculated with the same symmetries except  $13$  ( $C_s$ ) by the DFT. Additionally,  $11^+$  was optimized with restriction of the  $\text{C}-\text{Si}^+-\text{C}-\text{Si}$  dihedral angles of  $0^\circ$ ,  $30^\circ$ ,  $60^\circ$ , and  $90^\circ$ . Computed geometries were verified by frequency calculations. Furthermore, global minima were checked by manually changing initial geometries and by comparing the resulting optimized structures and their energies.

The structure of  $5^+$  with  $C_{3v}$  symmetry was calculated to be a transition state and less stable than a slightly twisted structure with  $C_3$  symmetry. Structures  $14^+$  and  $14$  with  $C_1$  symmetry were found to be more stable than those with  $C_s$  symmetry.

NMR chemical shifts were calculated by the GIAO methods at the B3LYP/6-31G(d,p)//B3LYP/6-31G(d,p) level and were referenced to TMS (molecular point group  $T_d$ ; calculated isotropic magnetic shielding constant 424.5;  $\delta^{29}\text{Si} = 0.0$ ). Table 1 summarizes the total energies ( $E$ ), zero-point energies (ZPE), and Gibbs free energies ( $G$ ) for the silylium cations studied in this work (also listed are the  $\Delta G$  and  $\Delta\Delta G$  values; both in kcal/mol). The energies for the corresponding silane neutrals ( $E$ , ZPE, and  $G$ ) are provided in Table S1 (Supporting Information). The computed GIAO NMR chemical shifts and their changes relative to neutral silane precursors are gathered in charts for each group of silylium ions. Geometries, the MKS and NPA charges, and changes in charges are collected in charts in the Supporting Information.

**On the Reliability of the Computed  $^{29}\text{Si}$  NMR Chemical Shifts.** Using IGLO II//B3LYP/6-31G\*, Olah and associates<sup>11</sup> reported  $\text{Me}_3\text{Si}^+$  at 354.2 ppm and  $\text{Et}_3\text{Si}^+$  at 371.3 ppm. On the basis of the geometries optimized at the HF/6-31G(d) level, Reed and co-workers<sup>12</sup> estimated the  $^{29}\text{Si}$  chemical shifts for  $\text{Me}_3\text{Si}^+$  at 354 (GIAO) and 382 (SOS-DFPT) ppm, and for  $\text{Et}_3\text{Si}^+$  at 371.2 (GIAO) and 415.6 (SOS-DFPT) ppm, respectively. According to Cremer and associates<sup>13</sup> the  $^{29}\text{Si}$  chemical shift (SOS-DFPT method) for  $\text{Me}_3\text{Si}^+$  is at 381.8 ppm. At the GIAO/B3LYP/6-31G(d,p)//B3LYP/6-31G(d,p) level employed in the present study, we obtained the following:  $\text{Me}_3\text{Si}^+$  at 389.3 ppm and  $\text{Et}_3\text{Si}^+$  at 417.0 ppm. These values are close to those obtained with SOS-DFPT, demonstrating that the level is adequate, especially given the comparative nature of the present investigation.

## Definition of Pyramidalization Angle ( $\theta_P$ ) for the $\text{Si}^+$ Atoms and Dihedral Angles ( $\theta$ ) between p-

(10) Frisch, M. J.; Trucks, G. W.; Schlegel, H. B.; Scuseria, G. E.; Robb, M. A.; Cheeseman, J. R.; Zakrzewski, V. G.; Montgomery, J. A. Jr.; Stratmann, R. E.; Burant, J. C.; Dapprich, S.; Millam, J. M.; Daniels, A. D.; Kudin, K. N.; Strain, M. C.; Farkas, O.; Tomasi, J.; Barone, V.; Cossi, M.; Cammi, R.; Mennucci, B.; Pomelli, C.; Adamo, C.; Clifford, S.; Ochterski, J.; Petersson, G. A.; Ayala, P. Y.; Cui, Q.; Morokuma, K.; Malick, D. K.; Rabuck, A. D.; Raghavachari, K.; Foresman, J. B.; Cioslowski, J.; Ortiz, J. V.; Baboul, A. G.; Stefanov, B. B.; Liu, G.; Liashenko, A.; Piskorz, P.; Komaromi, I.; Gomperts, R.; Martin, R. L.; Fox, D. J.; Keith, T.; Al-Laham, M. A.; Peng, C. Y.; Nanayakkara, A.; Challacombe, M.; Gill, P. M. W.; Johnson, B.; Chen, W.; Wong, M. W.; Andres, J. L.; Gonzalez, C.; Head-Gordon, M.; Replogle, E. S.; Pople, J. A. *Gaussian 98*, Revision A.9; Gaussian, Inc.: Pittsburgh, PA, 1998.

(11) Olah, G. A.; Rasul, G.; Prakash, G. K. S. *J. Organomet. Chem.* **1996**, *521*, 271.

(12) Xie, Z.; Manning, J.; Reed, R. W.; Mathur, R.; Boyd, P. D. W.; Benesi, A.; Reed, C. A. *J. Am. Chem. Soc.* **1996**, *118*, 2922.

(13) Kraka, E.; Sosa, C. P.; Gräfenstein, J.; Cremer, D. *Chem. Phys. Lett.* **1997**, *279*, 9.

**TABLE 1.** Electronic Energies (*E*), Zero-Point Energies (ZPE), and Gibbs Free Energies (*G*) Obtained from DFT Calculations (B3LYP/6-31G(d,p)//B3LPY(6-31G(d,p))

compd	<i>E</i> , hartree	ZPE, hartree	<i>G</i> , hartree	$\Delta G$ , kcal/mol <sup>a</sup>	$\Delta\Delta G$ , kcal/mol
<b>1<sup>+</sup></b>	-641.2556575	0.224151	-641.062536	548.3	(0)
<b>2-Me<sup>+</sup></b>	-932.0052435	0.242243	-931.798643	540.1	-8.2 <sup>b</sup>
<b>2-F<sup>+</sup></b>	-991.9710730	0.208162	-991.797533	549.1	0.8 <sup>b</sup>
<b>2-Cl<sup>+</sup></b>	-1352.3147568	0.207007	-1352.143336	549.9	1.6 <sup>b</sup>
<b>2-Br<sup>+</sup></b>	-3463.8348632	0.206653	-3463.664801	548.2	0.1 <sup>b</sup>
<b>3-Me<sup>+</sup></b>	-1222.7654372	0.260462	-1222.543950	533.2	-15.1 <sup>b</sup>
<b>4-Me<sup>+</sup></b>	-1513.5339590	0.278453	-1513.296901	526.8	-21.5 <sup>b</sup>
<b>5<sup>+</sup></b>	-563.8114995	0.186933	-563.656447	551.5	(0)
<b>6<sup>+</sup></b>	-893.8873211	0.232690	-893.692811	540.9	-10.6 <sup>c</sup>
<b>5a<sup>+</sup></b>	-603.1526043	0.214183	-602.972585	540.5	(0)
<b>6a<sup>+</sup></b>	-893.8942324	0.232068	-893.699693	536.9	-3.6 <sup>d</sup>
<b>7<sup>+</sup></b>	-524.4770887	0.157857	-524.349807	559.4	(0)
<b>8<sup>+</sup></b>	-854.5557245	0.203708	-854.388100	546.8	-12.6 <sup>e</sup>
<b>9<sup>+</sup></b>	-525.7363110	0.177127	-525.593605	542.7	(0)
<b>10<sup>+</sup></b>	-855.8053372	0.223325	-855.622003	536.0	-6.7 <sup>f</sup>
<b>11<sup>+</sup></b>	-817.7057444	0.212735	-817.535799	534.6	
<b>12<sup>+</sup></b>	-717.7413880	0.250082	-717.527039	-200.2	
<b>13<sup>+</sup></b>	-757.0531935	0.279360	-756.812270	-206.7	
<b>14<sup>+</sup></b>	-1008.4847689	0.267981	-1008.255477	-204.1	

<sup>a</sup> For each silylum ion Gibbs free energies are relative to Gibbs free energies for neutral silanes, silanols, or silyl ether. <sup>b</sup> Relative  $\Delta G$  to  $\Delta G$  for **1<sup>+</sup>**. <sup>c</sup> Relative  $\Delta G$  to  $\Delta G$  for **5<sup>+</sup>**. <sup>d</sup> Relative  $\Delta G$  to  $\Delta G$  for **5a<sup>+</sup>**. <sup>e</sup> Relative  $\Delta G$  to  $\Delta G$  for **7<sup>+</sup>**. <sup>f</sup> Relative  $\Delta G$  to  $\Delta G$  for **9<sup>+</sup>**.

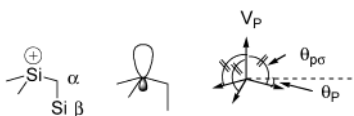


**FIGURE 4.** The vacant p-orbital axis vector ( $\mathbf{V}_p$ ), which makes equal angles ( $\theta_{p\sigma}$ ) to the three  $\sigma$ -bonds at the  $\text{Si}^+$  atom, and pyramidalization angle  $\theta_p = (\theta_{p\sigma} - 90)^\circ$ .

**Orbitals of  $\text{Si}^+$  and  $\text{C}(\alpha)-\text{Si}(\beta)$  Bonds.** We have adopted Haddon's p-orbital axis vector (POAV) analysis concept,<sup>13</sup> which was used for geometrical analysis of the structures of bridged [10]annulenes, to define and quantify the pyramidalization angle in the silylum ions in the present study. In this treatment the vacant p-orbital axis vector ( $\mathbf{V}_p$ ) of the  $\text{Si}^+$  atom is defined as that vector which makes equal angles ( $\theta_{p\sigma}$ ) to the three  $\sigma$ -bonds at the  $\text{Si}^+$  atom, and the pyramidalization angle is obtained as  $\theta_p = (\theta_{p\sigma} - 90)^\circ$ . A dihedral angle ( $\phi$ ) between the p-orbital of  $\text{Si}^+$  and the  $\text{C}(\alpha)-\text{Si}(\beta)$  bond is defined by using this hypothetical p-orbital axis vector ( $\mathbf{V}_p$ ) (Figure 4).

**1-Silaadamant-1-yl Cation and  $\beta$ -Silyl-Substituted 1-Silaadamant-1-yl Cations. (a) Optimized Geometries and Relative Energies (Chart S1 and Table 1).** The parent 1-silaadamant-1-yl cation (**1<sup>+</sup>**) has  $C_{3v}$  symmetry, the bridgehead Si atom is pyramidalized by  $16.3^\circ$  ( $\theta_p$ ), and the p-orbital of  $\text{Si}^+$  is parallel to  $\text{C}(\alpha)-\text{C}(\beta)$  bonds ( $\phi = 0^\circ$ ). The  $\text{Si}-\text{C}(2)$  bond is shorter and the  $\text{C}(2)-\text{C}(3)$  bond is longer relative to the silane precursor (Si-H compound **1**). Introduction of the  $\beta$ -SiMe group (**2-Me<sup>+</sup>**) decreases the pyramidalization angle at the silylum ion. At the same time, shortening of the  $\text{Si}^+-\text{C}(2)$  and lengthening of the  $\text{C}(2)-\text{Si}(3)$  bonds (relative to corresponding neutral silane **2**) become more pronounced. The observed changes suggest that the  $\beta$ -silyl effect is larger than a  $\beta$ -alkyl in the silaadamantyl cation, which parallels the known  $\beta$ -silyl versus  $\beta$ -alkyl stabilization in carbenium ions.<sup>2</sup> Sequential introduction of the  $\beta$ -SiMe groups into **1<sup>+</sup>** (**2-Me<sup>+</sup>** through **4-Me<sup>+</sup>**) stabilizes the silylum ion by 8.2, 15.1, and 21.5 kcal/mol, respectively (Table 1). The observed changes in  $\text{Si}-\text{C}(2)$

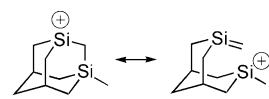


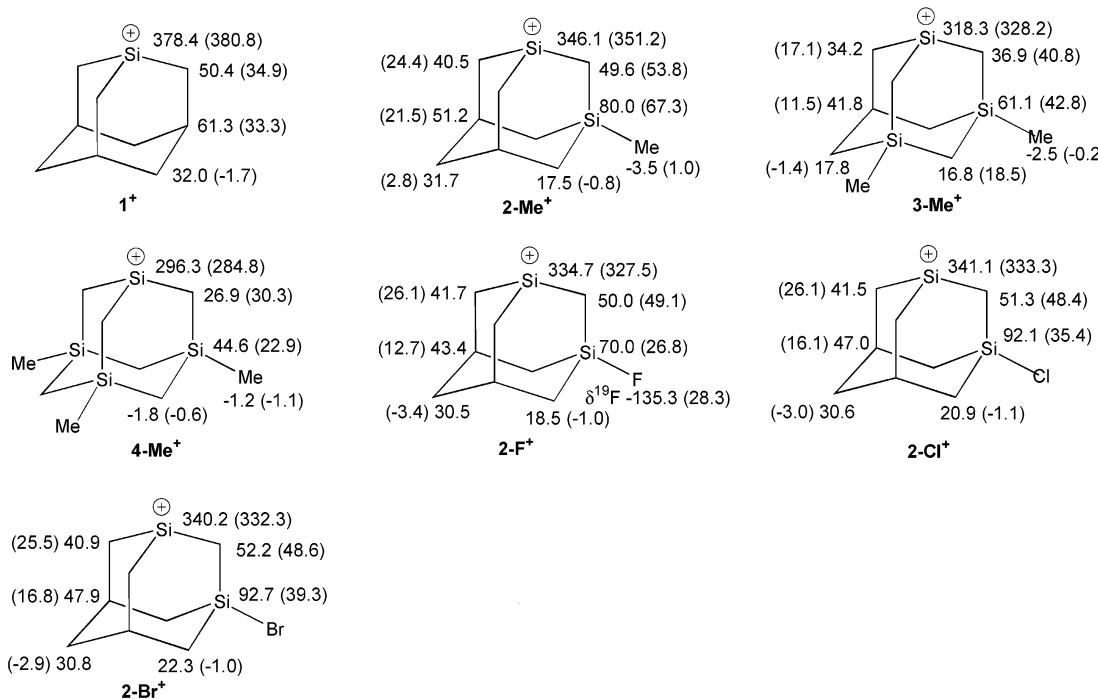
**FIGURE 5.** Hyperconjugation in **2-Me<sup>+</sup>**.

and  $\text{C}(2)-\text{Si}(3)$  bond lengths are proportional to the number of  $\beta$ -SiMe groups participating in hyperconjugative stabilization (as in Figure 5). Silylum ion **4-Me<sup>+</sup>** exhibits the smallest degree (10.8°) of silicon pyramidalization in this group. Although based on geometrical considerations hyperconjugation is also evident in the  $\beta$ -SiX-substituted silylum ions **2-F<sup>+</sup>**, **2-Cl<sup>+</sup>**, and **2-Br<sup>+</sup>**, the stabilization effect ( $-\Delta\Delta G$ ) has noticeably diminished ( $-0.8$ ,  $-1.6$ , and  $-0.1$  kcal/mol, respectively, relative to **1<sup>+</sup>**).

**(b) GIAO NMR and Changes in MKS- and NPA-Derived Charges (Chart 1 and Charts S2 and S3).** The computed  $\delta^{29}\text{Si}$  for **1<sup>+</sup>** is 378.4 ppm and  $\Delta\delta^{29}\text{Si}$  is 380.8 ppm relative to silane **1**. The  $\Delta\delta^{13}\text{C}$  values for  $\text{C}(\alpha)$  and  $\text{C}(\beta)$  are about equal [ $\delta$  34.9 at  $\text{C}-2$  and  $\delta$  33.3 at  $\text{C}(3)$ ], even though  $\text{C}(3)$  is further away from the cationic center. The charge delocalization patterns that emerge based on computed MKS and NPA changes in charges are not identical; the former indicates that positive charge is localized on the  $\text{Si}^+$  and on the  $\beta$ -carbons, whereas the latter shows that positive charge is localized on  $\text{Si}^+$ .

In the  $\beta$ -silyl-substituted silylum ions the silicocation center is sequentially shielded as more  $\beta$ -silyl groups are introduced, while at the same time deshielding at individual  $\beta$ -Si centers decreases. The observed trends appear consistent with diminished electron demand at  $\text{Si}^+$  due to increased hyperconjugative stabilization. The  $\Delta\delta$  for  $\beta$ -Si in the  $\beta$ -SiX-substituted silylum ions increases in the order **2-F<sup>+</sup>** < **2-Cl<sup>+</sup>** < **2-Br<sup>+</sup>** and the  $\Delta\delta\text{Si}^+$  shows the trend **2-F<sup>+</sup>** < **2-Cl<sup>+</sup>** ~ **2-Br<sup>+</sup>**. The  $\text{C}(\alpha)$  and to a lesser extent  $\text{C}(\beta)$  are also deshielded. These trends seem to suggest that hyperconjugation by a  $\beta$ -SiF group is somewhat more effective as compared to  $\beta$ -SiCl or  $\beta$ -SiBr, but this was not born out by relative stabilization

**CHART 1. Computed GIAO NMR Chemical Shifts for **1<sup>+</sup>**, **2-Me<sup>+</sup>**, **3-Me<sup>+</sup>**, **4-Me<sup>+</sup>**, **2-F<sup>+</sup>**, **2-Cl<sup>+</sup>**, and **2-Br<sup>+</sup>** (changes of chemical shifts relative to silanes neutral precursors in parentheses)**



energies. A smaller  $\Delta\delta^{29}\text{Si}$  for  $\text{SiF}$  is presumably due to fluorine back-bonding, which is corroborated by fluorine deshielding ( $\Delta\delta^{19}\text{F} = 28.3$  ppm) and by  $\text{Si}-\text{F}$  bond shortening (by 0.400 Å), which is more pronounced relative to  $\text{Si}-\text{Cl}$  in **2-Cl<sup>+</sup>** (0.258 Å) and  $\text{Si}-\text{Br}$  in **2-Cl<sup>+</sup>** (0.206 Å).

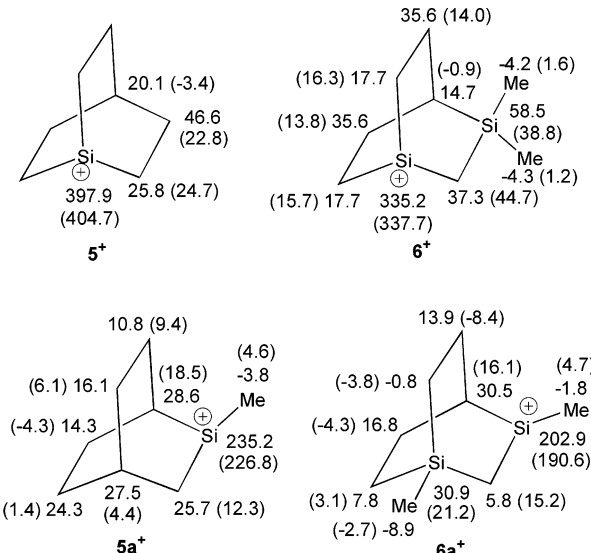
The MKS-derived changes in charges for **2-F<sup>+</sup>**, **2-Cl<sup>+</sup>**, and **2-Br<sup>+</sup>** show positive charge localization on  $\text{Si}^+$ ,  $\beta$ -Si, and  $\beta$ -Cs (Charts S2 and S3, Supporting Information), whereas the NPA-derived changes in charges imply heavy localization of positive charge on  $\text{Si}^+$ .

**Model Studies on Silabicyclo[2.2.2]octyl, Silanorbornyl, and Silacyclohexyl Cations.** To examine structural effects on relative stability and to probe the  $\beta$ -Si-C-Si<sup>+</sup> effect in other rigid cyclic systems for comparison with the 1-silaadamantyl cations discussed above, a series of silylum ions derived from silabicyclo[2.2.2]octyl, silanorbornyl, and silacyclohexyl cations was investigated.

**(a) 1-Silabicyclo[2.2.2]oct-1-yl (5<sup>+</sup>), 3,3-Dimethyl-1,3-disilabicyclo[2.2.2]oct-1-yl (6<sup>+</sup>), 2-Methyl-2-silabicyclo[2.2.2]oct-2-yl (5a<sup>+</sup>), and 1,3-Dimethyl-1,3-disilabicyclo[2.2.2]oct-3-yl (6a<sup>+</sup>) Cations (Chart 2 and Charts S4–S6).** The optimized structure of (5<sup>+</sup>) has  $C_3$  symmetry with a twist angle of 4.2° [ $\text{Si}-\text{C}(2)-\text{C}(3)-\text{C}(4)$ ]. The p-orbital at  $\text{Si}^+$  is nearly parallel to the  $\text{C}(\alpha)-\text{Si}(\beta)$  bonds (0.1° dihedral angle). The pyramidalization angle at  $\text{Si}^+$  is 15.0°. The cation has a shorter  $\text{Si}-\text{C}(2)$  bond and a longer  $\text{C}(2)-\text{C}(3)$  bond relative to neutral 1-silabicyclo[2.2.2]octane (5), indicative of  $\beta$ -C-C-Si<sup>+</sup> hyperconjugation. The computed  $\delta^{29}\text{Si}$  for 5<sup>+</sup> is 397.9, deshielded by 404.7 ppm from the silane precursor (5).

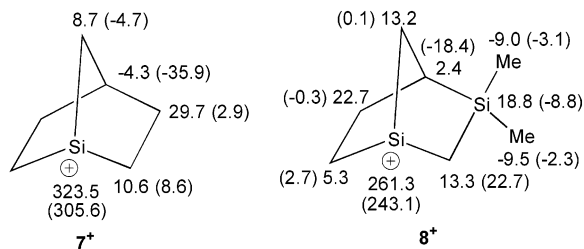
The  $\beta$ -silyl derivative, 3,3-dimethyl-1,3-disilabicyclo[2.2.2]oct-1-yl cation (6<sup>+</sup>), has close to  $C_s$  structure. The  $\text{Si}^+$  center is pyramidalized by 12.3° and the dihedral

**CHART 2. Computed GIAO NMR Chemical Shifts for **5<sup>+</sup>**, **6<sup>+</sup>**, **5a<sup>+</sup>**, and **6a<sup>+</sup>** (changes of chemical shifts relative to silane neutral precursors in parentheses)**



angle between the p-orbital of  $\text{Si}^+$  and  $\text{C}(\alpha)-\text{Si}(\beta)$  bonds is 0.0°. Introduction of the  $\beta$ -silyl group stabilizes the cation by 10.6 kcal/mol relative to 5<sup>+</sup>. It leads to shortening of the  $\text{Si}-\text{C}(2)$  and lengthening of the  $\text{C}(2)-\text{Si}(3)$  bonds. The  $\delta^{29}\text{Si}$  chemical shift moves to  $\delta$  335.2, deshielded by 337.7 ppm from the silane precursor (6). The  $\beta$ -silicon atom is deshielded by 38.8 ppm, which is noticeably less than that for 2-Me<sup>+</sup>. The  $\text{C}(\alpha)$  and  $\text{C}(\beta)$  carbons are both deshielded, whereas  $\text{C}(\gamma)$  is somewhat shielded. As observed with the silaadamantyl cations, the MKS-derived changes in charges in 5<sup>+</sup> and 6<sup>+</sup> place the positive charge on silicon(s) and on the  $\beta$ -carbons, whereas the

**CHART 3. Computed GIAO NMR Chemical Shifts for  $7^+$  and  $8^+$  (changes of chemical shifts relative to silane precursors in parentheses)**



NPA computed charge is heavily localized on the  $\text{Si}^+$  center.

In the silylum ions  $5\mathbf{a}^+$  and  $6\mathbf{a}^+$ , the  $\text{Si}^+$  center has been moved from a bridgehead to a nonbridgehead position. The  $\text{Si}^+$  is pyramidalized by  $4.0^\circ$  in  $5\mathbf{a}^+$  and by  $3.7^\circ$  in  $6\mathbf{a}^+$ . The dihedral angle between silicon p-orbital and the adjacent bond is  $50.3^\circ$  ( $\text{C}(3)-\text{C}(4)$ ) for  $5\mathbf{a}^+$  and  $74.3^\circ$  ( $\text{C}(2)-\text{Si}(1)$ ) for  $6\mathbf{a}^+$ . Such deviations from periplanar arrangement should diminish vertical stabilization. Indeed,  $6\mathbf{a}^+$  gains only moderate stability relative to  $5\mathbf{a}^+$  (3.6 kcal/mol). GIAO NMR predicts that moving the  $\text{Si}^+$  to a nonbridgehead position has a significant shielding effect. Thus  $\delta^{29}\text{Si}$  for  $5\mathbf{a}^+$  is computed at  $\delta$  235.2 ( $\Delta\delta = 226.8$  ppm). Hyperconjugation by  $\beta$ -silicon causes further shielding. Therefore, the  $\delta^{29}\text{Si}$  for  $6\mathbf{a}^+$  is at  $\delta$  202.9 ( $\Delta\delta = 190.6$  ppm). The  $\beta$ -silicon and two  $\alpha$ -carbons exhibit noticeable deshielding. For  $5\mathbf{a}^+$ , the MKS-derived changes in charges place positive charge on  $\text{Si}^+$  and on three  $\beta$ -carbons. In  $6\mathbf{a}^+$  positive charge resides on  $\text{Si}^+$ , on  $\beta$ -Si, and on two  $\beta$ -carbons. As in earlier examples, based on NPA analysis positive charge is heavily localized on  $\text{Si}^+$ .

**(b) The 1-Silanorborn-1-yl ( $7^+$ ) and 3,3-Dimethyl-1,3-disilanorbornyl ( $8^+$ ) Cations (Chart 3 and Charts S7–S9).** Silicon pyramidalization in the silanorbornyl cation ( $7^+$ ) is more pronounced relative to 1-silabicyclo[2.2.2]oct-1-yl cation ( $5^+$ ) ( $20.9^\circ$  versus  $15.0^\circ$ ). The p-orbital at  $\text{Si}^+$  and the  $\text{C}(2)-\text{C}(3)$  bond are forced out of periplanar arrangement (dihedral angle  $\phi = 17.2^\circ$ ). Moreover, the increase in  $\text{C}(2)-\text{C}(3)$  bond length has become less pronounced. The computed  $\delta^{29}\text{Si}$  chemical shift for  $7^+$  is  $\delta$  323.5 ( $\Delta\delta^{29}\text{Si} = 305.6$  ppm), which is noticeably more shielded relative to  $5^+$ . Introduction of the  $\beta$ -silyl group ( $8^+$ ) decreases the pyramidalization angle and the dihedral angle, and lowers the energy of the silylum ion by 12.6 kcal/mol. The  $\delta^{29}\text{Si}$  in  $8^+$  moves to  $\delta$  261.3, which is shielded by ca. 74 ppm relative to  $6^+$ . Interestingly, the  $\beta$ -silicon in  $8^+$  does not show deshielding (as was the case with  $5^+$ ), instead it is somewhat shielded. There is also relatively less deshielding at  $\text{C}(2)$  and more shielding at  $\text{C}(4)$ . These changes probably stem from through space orbital interactions in the more strained bicyclo[2.2.1]nonyl structure.<sup>15</sup> It is noteworthy that despite increased strain and a noticeable dihedral angle,  $\beta$ -silyl stabilization has a higher impact on  $7^+$  than on  $5^+$  (by 2 kcal/mol).

**(c) The 1-Methyl-1-silacyclohex-1-yl and 1,3,3-Trimethyl-1,3-disilacyclohex-1-yl Cations ( $9^+$  and**

**CHART 4. Computed GIAO NMR Chemical Shifts for  $9^+$  and  $10^+$  (changes of chemical shifts relative to silane precursors in parentheses)**

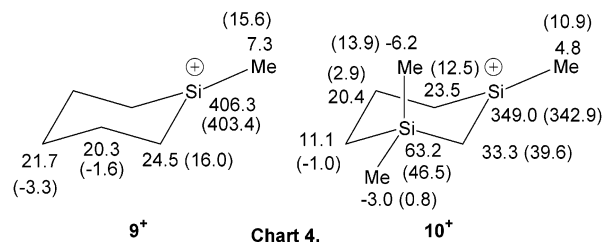


Chart 4.

$10^+$ ) (Chart 4 and Charts S10–S12). Whereas the pyramidalization angle for the silicon atom in  $9^+$  is very small ( $0.6^\circ$ ) the dihedral angle between the vacant p-orbital and  $\text{C}(2)-\text{C}(3)$  is quite substantial ( $78.2^\circ$ ). The computed silicon chemical shift for  $9^+$  is at  $\delta$  406.3 ( $\Delta\delta = 403.4$  ppm); both  $\text{C}(\alpha)$  and  $\text{Si}(Me)$  are deshielded relative to the silane precursor ( $9$ ). Introduction of the  $\beta$ -silyl substituent ( $10^+$ ) significantly reduces the dihedral angle ( $29.1^\circ$ ) while slightly increasing the  $\text{Si}^+$  pyramidalization angle ( $4.1^\circ$ ). Shortening of the  $\text{Si}(1)-\text{C}(2)$  and lengthening of the  $\text{C}(2)-\text{Si}(3)$  in  $10^+$  are also notable. The  $\text{Si}^+$  center becomes shielded (moves to  $\delta$  349.0 in  $10^+$ ) while the  $\beta$ -silyl group is deshielded relative to  $10$  by 46.5 ppm. The  $\text{C}(2)/\text{C}(6)$  are also deshielded. Introduction of the  $\beta$ -silyl substituent lowers the energy of the silylum ion by 6.7 kcal/mol.

**Dependence of the  $^{29}\text{Si}$  Chemical Shifts and Energies on the Dihedral Angle in 1,1,3,3-Tetramethyl-1,3-disilabut-1-yl cation ( $11^+$ ) (Chart 5 and Charts S13–S15).** The structure of 1,1,3,3-tetramethyl-1,3-disilabut-1-yl cation ( $11^+$ ) was optimized without restriction (A) or with a fixed dihedral angle ( $\phi$ ) of  $1.6^\circ$  (B),  $26.2^\circ$  (C),  $56.5^\circ$  (D), and  $90.0^\circ$  (E) between the vacant p-orbital of  $\text{Si}^+$  and the  $\text{C}(\alpha)-\text{Si}(\beta)$  bond (Chart 5). Total energies increase with increasing dihedral angles with a maximum energy difference of 5.9 kcal/mol. Vibrational analysis showed no imaginary frequency for the first three geometries and one imaginary frequency for the remaining structures. The  $\delta^{29}\text{Si}$  GIAO chemical shift data are 347.2 ( $1.6^\circ$ , A), 347.0 ( $1.6^\circ$ , B), 352.5 ( $26.2^\circ$ , C), 370.9 ( $56.5^\circ$ , D), and 388.7 ( $90.0^\circ$ , E), showing a shielding trend for the  $\text{Si}^+$  with increasing effectiveness for hyperconjugation via lowering of the dihedral angle. The relationship of the twist angle and energy is illustrated in Figure 6.

**Interaction of Silaadamantyl Cations with  $\text{H}_2\text{O}$  and  $\text{MeOH}$  (Chart 6, Figure S1, and Charts S16–S19).** The strong tendency of silylum ions to form complexes with various  $\pi$ - and n-donor solvents and to coordinate to inert species such as  $\text{CH}_4$  and even to noble gases is now well-established.<sup>16</sup> In solution, the incipient  $\text{R}_3\text{Si}^+$  reacts with ether solvents to form silyloxonium ions.<sup>17</sup> In the context of the present computational study, we also examined the interaction of 1-silaadamantyl

(14) Haddon, R. C. *J. Phys. Chem. A* **2001**, *105*, 4164. Haddon, R. C. *Acc. Chem. Res.* **1988**, *21*, 243.

(15) Martinez, A. G.; Teso Vilar, E.; Osio Barcina, J.; de la Moya Cerero, S. *J. Am. Chem. Soc.* **2002**, *124*, 6676.

(16) (a) Review: Maerker, C.; Kapp, J.; Schleyer, P. v. R. In *Organosilicon Chemistry II, From Molecules to Materials*; Auner, N., Weiss, J., Eds.; VCH: Weinheim, Germany, 1996; pp 329–359. (b) Olsson, L.; Ottosson, C.-H.; Cremer, D. *J. Am. Chem. Soc.* **1995**, *117*, 7460. (c) Ottosson, C.-H.; Szabo, K. J.; Cremer, D. *Organometallics* **1997**, *16*, 2377.

(17) Kira, M.; Hino, T.; Sakurai, H. *J. Am. Chem. Soc.* **1992**, *114*, 6697.

**CHART 5. Computed GIAO NMR Chemical Shifts for **11<sup>+</sup>** (A–E) (changes of chemical shifts relative to a silane precursor in parentheses)**

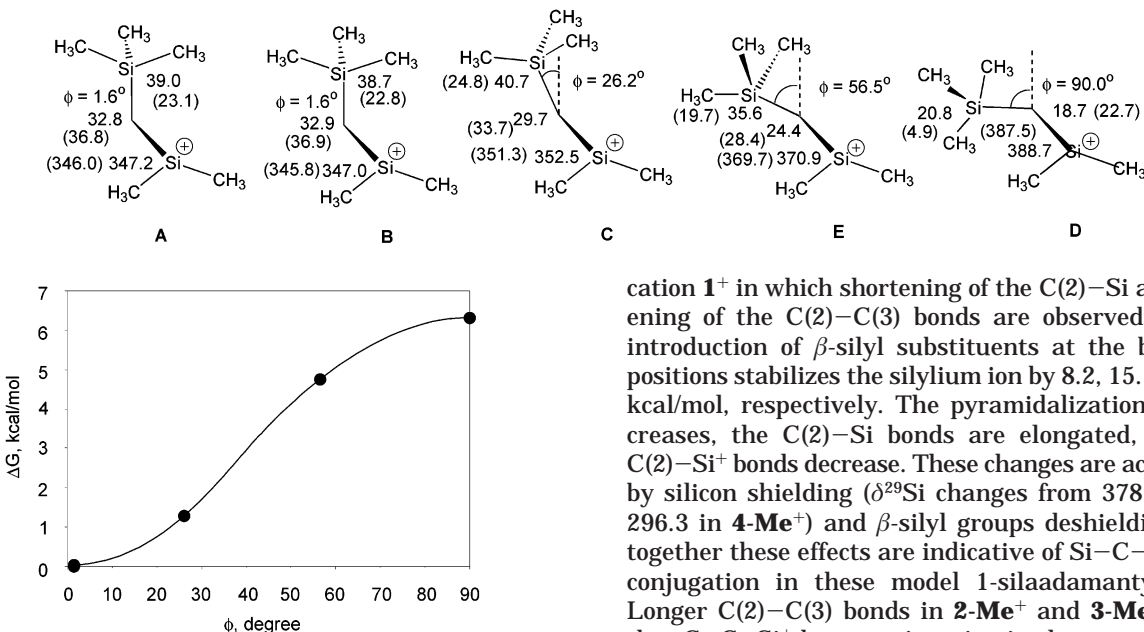


**FIGURE 6.** The relationship of the dihedral angle ( $\phi$ ) between the p-orbital of  $\text{Si}^+$  and the  $\text{C}(\alpha)\text{-Si}(\beta)$  bond and relative Gibbs free energy ( $\Delta G$ ) for **11<sup>+</sup>** by B3LYP/6-31G(d,p)//B3LYP/6-31G(d,p).

cation **1<sup>+</sup>** with  $\text{H}_2\text{O}$  and  $\text{MeOH}$  and its  $\beta$ -silyl-substituted derivative **2-Me<sup>+</sup>** with  $\text{H}_2\text{O}$ .

The global minimum in the reaction of **1<sup>+</sup>** with water (**12<sup>+</sup>**) has an  $\text{Si}-\text{O}$  bond length of  $1.917 \text{ \AA}$ , which is very close to that in  $\text{Me}_3\text{SiOH}_2^+$  reported by Olah et al.<sup>11</sup> The  $^{29}\text{Si}$  NMR chemical shift of **12<sup>+</sup>** is computed at  $118.4 \text{ ppm}$  (that of  $\text{Me}_3\text{SiOH}_2^+$  is at  $101.9 \text{ ppm}$ <sup>11</sup>). Optimization with restriction of the  $\text{Si}-\text{O}$  bond length between  $2$  and  $4 \text{ \AA}$  gave higher energy structures whose  $\delta^{29}\text{Si}$  varied between  $139.0$  and  $367.3 \text{ ppm}$ , respectively (variation of  $\text{O}-\text{Si}$  bond length vs energy for **12<sup>+</sup>** and **14<sup>+</sup>** is plotted in Figure S1).

Reaction of **1<sup>+</sup>** with  $\text{MeOH}$  gave the silaoxonium ion **13<sup>+</sup>**, with an  $\text{Si}-\text{O}$  bond length of  $1.873 \text{ \AA}$  and a silicon chemical shift of  $104.5 \text{ ppm}$ . Reaction of the  $\beta$ -silyl-substituted silylium ion **2-Me<sup>+</sup>** with  $\text{H}_2\text{O}$  gave **14<sup>+</sup>** as a global minimum. The  $\text{Si}-\text{O}$  bond length is  $1.932 \text{ \AA}$  and the  $^{29}\text{Si}$  chemical shifts are  $121.1$  and  $32.3 \text{ ppm}$ . Increasing the  $\text{O}-\text{Si}$  bond length produced higher energy structures and no other minima were found. The optimized structures exhibited  $\delta^{29}\text{Si}$  of  $137.0 \text{ ppm}$  at the  $\text{Si}-\text{O}$  bond distance of  $2.0 \text{ \AA}$ ,  $244.8 \text{ ppm}$  at  $2.5 \text{ \AA}$ , and  $336.6 \text{ ppm}$  at  $4.0 \text{ \AA}$ . The computed  $\Delta\delta^{29}\text{Si}$  values (relative to neutral silanols or the silyl ether) for **12<sup>+</sup>**, **13<sup>+</sup>**, and **14<sup>+</sup>** are  $95.1$ ,  $80.9$ , and  $91.4 \text{ ppm}$  with changes in the  $\text{Si}-\text{O}$  bond lengths of  $0.243$ ,  $0.203$ , and  $0.255 \text{ \AA}$  respectively. A slight increase in the  $\text{Si}(1)-\text{C}(\alpha)$  bond length and decrease in the  $\text{C}(\beta)-\text{C}(\gamma)$  and  $\text{C}(\beta)-\text{Si}(\gamma)$  bond lengths are noted which suggest some degree of hyperconjugative stabilization. The  $\delta^{29}\text{Si}$  values for the  $\beta$ -silicon also increase to some extent.

### Comparative Discussion

The  $\text{C}-\text{C}-\text{Si}^+$  hyperconjugation is manifested in the DFT optimized geometry of parent 1-silaadamantyl

cation **1<sup>+</sup>** in which shortening of the  $\text{C}(2)-\text{Si}$  and lengthening of the  $\text{C}(2)-\text{C}(3)$  bonds are observed. Stepwise introduction of  $\beta$ -silyl substituents at the bridgehead positions stabilizes the silylium ion by  $8.2$ ,  $15.1$ , and  $21.5 \text{ kcal/mol}$ , respectively. The pyramidalization angle decreases, the  $\text{C}(2)-\text{Si}$  bonds are elongated, while the  $\text{C}(2)-\text{Si}^+$  bonds decrease. These changes are accompanied by silicon shielding ( $\delta^{29}\text{Si}$  changes from  $378.4$  in **1<sup>+</sup>** to  $296.3$  in **4-Me<sup>+</sup>**) and  $\beta$ -silyl groups deshielding. Taken together these effects are indicative of  $\text{Si}-\text{C}-\text{Si}^+$  hyperconjugation in these model 1-silaadamantyl cations. Longer  $\text{C}(2)-\text{C}(3)$  bonds in **2-Me<sup>+</sup>** and **3-Me<sup>+</sup>** indicate that  $\text{C}-\text{C}-\text{Si}^+$  hyperconjugation is also operating; however, geometrical comparison with **1<sup>+</sup>** and taking into account the magnitude of  $\Delta\delta^{13}\text{C}$  at  $\text{C}(\beta)$  leads to the conclusion that the dominant stabilization factor is  $\text{Si}-\text{C}-\text{Si}^+$  hyperconjugation. The computed zero dihedral angle and reduced silicon pyramidalization should maximize vertical stabilization in these systems. When the  $\beta$ -silyl group is  $\text{SiX}$  instead of  $\text{SiMe}$ , the stabilization effect diminishes even though the changes in  $\text{C}(2)-\text{Si}^+$  and  $\text{C}(2)-\text{Si}$  bonds are similar. In the case of  $\text{X} = \text{Cl}$ , energy is lowered by  $1.6 \text{ kcal/mol}$ . In going from **2-F<sup>+</sup>** to **2-Cl<sup>+</sup>**, the  $\Delta\delta^{29}\text{Si}$  increases at both  $\text{Si}^+$  and  $\text{SiX}$ . Shortening of the  $\text{Si}-\text{F}$  bond implies fluorine back-bonding, which in turn could reduce deshielding at the  $\beta$ -silicon. Fluorine deshielding is indeed predicted ( $\Delta\delta^{19}\text{F} = 28.3 \text{ ppm}$ ). The  $\Delta\delta^{29}\text{Si}$  for the  $\text{Si}^+$  in **2-F<sup>+</sup>** is  $24 \text{ ppm}$  smaller than that for **2-Me<sup>+</sup>** and the  $\Delta\delta^{29}\text{Si}$  of  $\text{Si}(\beta)$  is also smaller. Taken together these findings support back-bonding via fluorine. Introduction of a  $\beta$ - $\text{SiMe}_2$  group into the 1-silabicyclo[2.2.2]octyl cation (**5<sup>+</sup>** to **6<sup>+</sup>**) lowers the energy of the silylium ion by  $10.6 \text{ kcal/mol}$ . The  $\text{Si}^+$  center is shielded and the  $\beta$ -silicon atom is deshielded. Positive charge resides predominantly on the cation center and on the  $\beta$ -carbons. Moving the  $\text{Si}^+$  from the bridgehead to a nonbridgehead position (**5a<sup>+</sup>**) has a shielding effect on the silylium ion. Introduction of a  $\beta$ -silyl group (as in **6a<sup>+</sup>**) shields the  $\text{Si}^+$  while deshielding the  $\beta$ -silicon. There is significant deviation from the peri-planar arrangement, and silicon pyramidalization also increases. These geometrical features lower the  $\beta$ -silyl-stabilization effect ( $3.6 \text{ kcal/mol}$ ).

The  $\text{Si}^+$  center in the silanorbornyl cation **7<sup>+</sup>** is more shielded than that in the silabicyclo[2.2.2]octyl cation **5<sup>+</sup>**. Introduction of the  $\beta$ -silyl group lowers the energy of the silylium ion by  $12.6 \text{ kcal/mol}$ . Shielding of the  $\text{Si}^+$  and deshielding of  $\beta$ -silicon are again observed. Among the studied silylium ions, the  $\text{Si}^+$  center in **9<sup>+</sup>** is computed to be most downfield. Introduction of the  $\beta$ -silyl group (**10<sup>+</sup>**) induces rather significant changes in the dihedral

**CHART 6. Computed GIAO NMR Chemical Shifts for  $12^+$ ,  $13^+$ , and  $14^+$  (changes of chemical shifts relative to silane precursors in parentheses)**

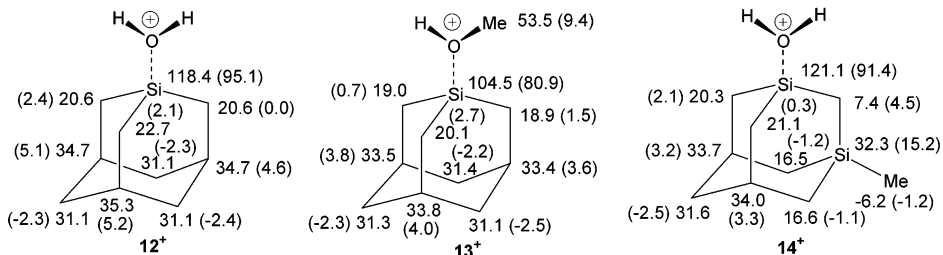


**TABLE 2. Computed  $\delta^{29}\text{Si}$  Data for the  $\text{Si}^+$  Atoms in  $1^+$ ,  $5^+$ ,  $5\text{a}^+$ ,  $7^+$ , and  $9^+$  and Their Pyramidalization Angles ( $\theta_P$ ) at the B3LYP/6-31G(d,p)//B3LYP(6-31G(d,p) Level**

cation	system	$\delta^{29}\text{Si}$	pyramidalization angles ( $\theta_P$ ), deg
<b>1<sup>+</sup></b>	1-silaamandant-1-yl	347.4	16.3
<b>5<sup>+</sup></b>	1-silabicyclo[2.2.2]oct-1-yl	397.9	15.0
<b>5a<sup>+</sup></b>	2-silabicyclo[2.2.2]oct-2-yl	235.2	4.0
<b>7<sup>+</sup></b>	1-silanorborn-1-yl	323.5	20.9
<b>9<sup>+</sup></b>	1-silacyclohex-1-yl	406.3	0.6

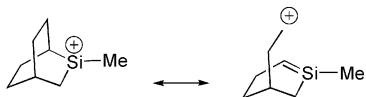


**FIGURE 7. Hyperconjugation in  $5\text{a}^+$ .**

angle and in silicon pyramidalization. The  $\beta$ -silyl stabilization effect in this case is 6.7 kcal/mol.

Computational study of model acyclic system  $11^+$  shows that as in the case of  $\text{Si}-\text{C}-\text{C}^+$  hyperconjugation, a parallel arrangement (zero twist angle) between the p-orbital at  $\text{Si}^+$  and the  $\text{Si}-\text{C}$   $\sigma$  bond maximizes stabilization via  $\text{Si}-\text{C}-\text{Si}^+$  hyperconjugation.

Table 2 provides a comparison of the  $^{29}\text{Si}$  NMR chemical shifts for the silylum ions which lack a  $\beta$ -silyl group. It can be seen that increased pyramidalization at silicon lowers the  $\delta^{29}\text{Si}$  value, except in  $5\text{a}^+$ , which is not a bridgehead cation. In the latter, the cationic Si orbital appears to be more stabilized by C–C hyperconjugation (as in Figure 7) than in other silylum cations.

The DFT-optimized structures of the cations resulting from reaction of  $\text{H}_2\text{O}$  and  $\text{MeOH}$  with  $1^+$  and  $\text{H}_2\text{O}$  with  $2\text{-Me}^+$  ( $12^+$ ,  $13^+$ ,  $14^+$ ) and their computed GIAO NMR chemical shifts are most consistent with the formation of silaoxonium ions, in concert with Olah et al.'s previous computational study of representative acyclic silylum ions with water and other n-donor as well as  $\pi$ -donor solvents.<sup>11</sup>

Finally, the MKS- and NPA-derived changes in charges for the studied silylum ions did not produce analogous patterns. Overall, the MKS-derived changes in charges appear more closely compatible with the GIAO-derived  $\Delta\delta$  values.

In conclusion, the  $\beta$ -silyl-stabilization effect on silylum cation (the  $\text{Si}-\text{C}-\text{Si}^+$  hyperconjugation) has been probed computationally in a series of caged, bicyclic, and monocyclic silylum ions through a combination of geometrical changes, energies, and the NMR chemical shift changes.

**Supporting Information Available:** Cartesian coordinates for the optimized structures of the studied silylum ions ( $1^+–14^+$ ) and their neutral silane precursors ( $1–14$ ); table of energies for the silane precursors ( $1–14$ ); charts of optimized geometries and computed MKS- and NPA-derived charges and changes in charges relative to silane precursors for each group of silylum ions ( $1^+–14^+$ ); plot of variation in O–Si bond length versus energy in  $12^+$  and  $14^+$ . This material is available free of charge via the Internet at <http://pubs.acs.org>.

JO026312X